Oceanology International 96
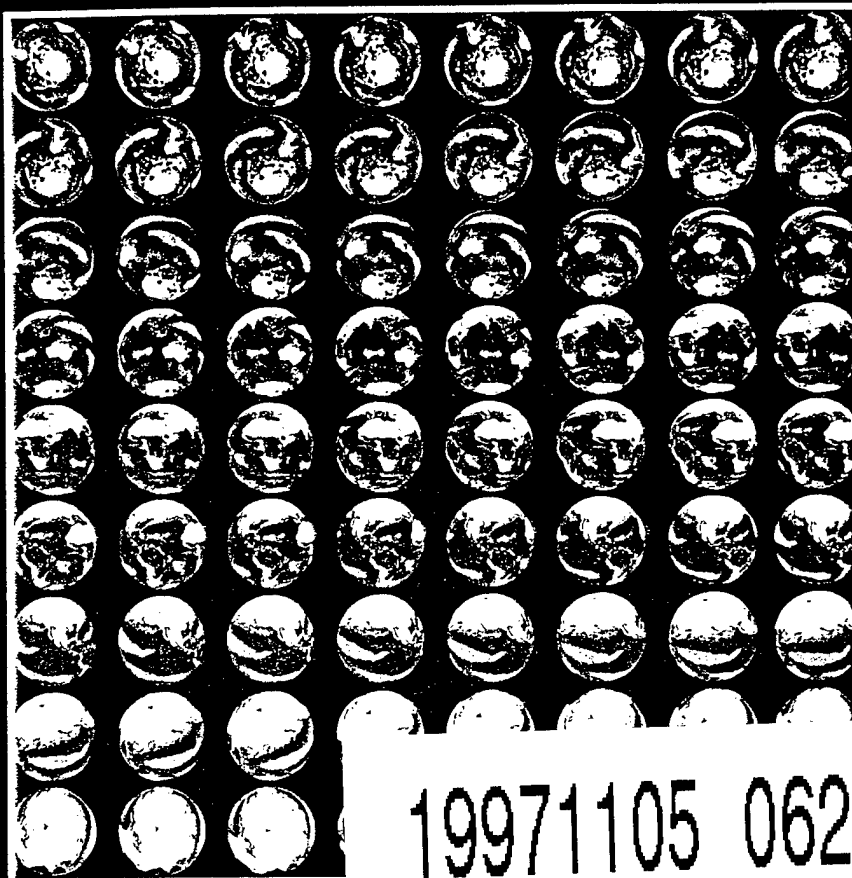
CONFERENCE PROCEEDINGS
VOLUME 1

5 - 8 March 1996 • Brighton, UK

REPORT DOCUMENTATION PAGE

Form Approved
OBM No. 0704-0188

Public reporting burden for this collection of information is estimated to average 1 hour per response, including the time for reviewing instructions, searching existing data sources, gathering and maintaining the data needed, and completing and reviewing the collection of information. Send comments regarding this burden or any other aspect of this collection of information, including suggestions for reducing this burden, to Washington Headquarters Services, Directorate for information Operations and Reports, 1215 Jefferson Davis Highway, Suite 1204, Arlington, VA 22202-4302, and to the Office of Management and Budget, Paperwork Reduction Project (0704-0188), Washington, DC 20503.

1. AGENCY USE ONLY *(Leave blank)*	2. REPORT DATE March 1996	3. REPORT TYPE AND DATES COVERED Proceedings

4. TITLE AND SUBTITLE

Environmental Factors Affecting the Acoustic Resonant Frequency Due to Internal Solitons

6. AUTHOR(S)

Michael K. Broadhead and Robert L. Field

5. FUNDING NUMBERS

Job Order No.   71668006

Program Element No. 062435N

Project No.

Task No.

Accession No.

7. PERFORMING ORGANIZATION NAME(S) AND ADDRESS(ES)

Naval Research Laboratory
Center for Environmental Acoustics
Stennis Space Center, MS 39529-5004

8. PERFORMING ORGANIZATION REPORT NUMBER

NRL/PP/7173--96-0001

9. SPONSORING/MONITORING AGENCY NAME(S) AND ADDRESS(ES)

Naval Research Laboratory
4555 Overlook Avenue, S.W.
Washington, DC 20375-5320

10. SPONSORING/MONITORING AGENCY REPORT NUMBER

12a. DISTRIBUTION/AVAILABILITY STATEMENT

Approved for public release; distribution is unlimited.

12b. DISTRIBUTION CODE

13. ABSTRACT *(Maximum 200 words)*

   Nonlinear shallow water internal waves can enhance the bottom interaction of underwater sound. For a lossy ocean bottom, this has the effect of an overall level change (in addition to fluctuations) in the transmission loss at preferred ("resonant") frequencies. The mechanism for this effect is acoustic mode coupling due to the depression of higher sound speed water into lower speed water (at the pycnocline). It is also possible for this mechanism to induce a transfer of acoustic energy from below the thermocline into the mixed layer, and we concentrate on this scenario. One of the environmental effects on the length scale of the internal wave packet has been shown to be dissipation. The effect of this scale broadening on the resonant frequency is studied. Through rigorous simulations, it is shown that this effect produces a positive shift in the frequency line structure. Also offered is a simple model for this effect, based on mode coupling theory, that qualitatively predicts several features observed in the simulations.

DTIC QUALITY INSPECTED 2

14. SUBJECT TERMS

acoustics, resonant frequency, internal solitons, internal waves, shallow water, lossy ocean bottom, transmission loss, pycnocline, thermocline, scale broadening, and mode coupling

15. NUMBER OF PAGES
9

16. PRICE CODE

17. SECURITY CLASSIFICATION OF REPORT Unclassified	18. SECURITY CLASSIFICATION OF THIS PAGE Unclassified	19. SECURITY CLASSIFICATION OF ABSTRACT Unclassified	20. LIMITATION OF ABSTRACT SAR

ENVIRONMENTAL FACTORS AFFECTING THE ACOUSTIC RESONANT FREQUENCY DUE TO INTERNAL SOLITONS

Michael K. Broadhead and Robert L. Field
Research Physicists

Naval Research Laboratory
Stennis Space Center, MS 39529
U. S. A.

Abstract

Nonlinear shallow water internal waves can enhance the bottom interaction of underwater sound. For a lossy ocean bottom, this has the effect of an overall level change (in addition to fluctuations) in the transmission loss at preferred ("resonant") frequencies. The mechanism for this effect is acoustic mode coupling due to the depression of higher sound speed water into lower speed water (at the pycnocline). It is also possible for this mechanism to induce a transfer of acoustic energy from below the thermocline into the mixed layer, and we concentrate on this scenario. One of the environmental effects on the length scale of the internal wave packet has been shown to be dissipation. The effect of this scale broadening on the resonant frequency is studied. Through rigorous simulations, it is shown that this effect produces a positive shift in the frequency line structure. Also offered is a simple model for this effect, based on mode coupling theory, that qualitatively predicts several features observed in the simulations.

Introduction

Zhou, *et al.* [1] have shown that nonlinear shallow water internal waves (IW's) can enhance the bottom interaction of underwater sound. For a lossy ocean bottom, this has the effect of an overall level change (in addition to fluctuations) in the transmission loss at preferred frequencies. These IW's can induce the coupling of lower-order to higher-order modes, allowing more acoustic energy to penetrate into the lossy sediments.

Broadhead [2] also found that an IW induced transfer of acoustic energy from below the thermocline into the mixed layer, in an idealized shallow water waveguide, could also occur. Over the frequency range studied (900 Hz -- 1030 Hz), the energy transfer spectrum exhibited a doublet resonant structure. At both resonant frequencies, mode coupling induced by the presence of internal waves was responsible for the effect. Inclusion of dissipative effects on the IW's revealed that the rate of wave packet spreading was reduced, and that soliton broadening accompanied amplitude reduction. It was found that the latter effect produced a positive shift in the resonant frequency structure.

In the present work, mode coupling theory has been used to produce a simple model of the connection between acoustic resonance frequencies and internal wave length scale. This model, which explicitly includes the various acoustical environmental parameters, qualitatively correctly predicts two of the effects we observed in simulations; namely, 1) an increase in acoustic resonant frequency with an increase in the IW length scale, and 2) prediction of a multiplet line structure, due to a generally unique resonant frequency being associated with each (m,n) mode pair.

Internal Wave Properties and Simulation

For summer conditions in shallow water, there is typically a mixed layer of warm, less dense water overlaying a colder, denser layer. The density contrast is small (on the order of 10^{-3} g/cm^3) and due mostly to temperature difference. However, because of the low compressibility of water, this small difference is sufficient to support internal waves (interface

waves along the pycnocline) of significant amplitude; usually on the order of tens of meters. Perturbation theory for shallow water conditions ($\lambda_{int} \gg H$) leads to the KdV equation [3]. Here, H refers to total fluid thickness and λ_{int} is the characteristic length scale of the IW's (refer to Fig. 1). The wave amplitude must be small (but finite) with respect to H for perturbation theory to be valid.

After Ostrovsky [3], we can write the KdV equation in the form appropriate for two-layer conditions:

$$u_t + cu_x + \alpha uu_x + \beta u_{xxx} = 0 \qquad\qquad 1)$$

where $u(x,t)$ is the displacement of the pycnocline from equilibrium level. The KdV coefficients are defined as follows: c is the linear phase speed, α is the nonlinear coefficient, β is the dispersion coefficient (refer to [3] for the full expressions for these quantities). If a traveling wave solution is assumed the KdV equation can be directly integrated to yield the sech-squared solitary wave solution:

$$u(x,t) = u_0 sech^2(\frac{x-Vt}{\Delta}), \qquad\qquad 2)$$

where V is the soliton velocity, Δ is the soliton half width,

$$V = c + \frac{\alpha u_0}{3}, \qquad\qquad 3)$$
and

$$\Delta^2 = \frac{12\beta}{\alpha u_0}. \qquad\qquad 4)$$

The solitons are waves of depression if $\rho_2 h_1^2 < \rho_1 h_2^2$, where ρ_1, ρ_2 are the densities of upper and lower layers, respectively, and h_1, h_2 are layer thicknesses. For use in simulations, we chose parameters for shallow water similar to Zhou's Yellow Sea case. The length scale of the main solitary wave is ~150 m, with an amplitude of ~10 m.

Dissipative Mechanisms in Shallow Water IWs

To study the effects of a dynamic environment on the IW's in such a way that the subsequent acoustical properties were affected, we were led to consider dissipative effects. Shear-induced turbulent dissipation, frictional drag in the bottom boundary layer, radial spreading, and coupling into other scales of wave motion (such as barotropic components) are some of the major sources of energy loss from the solitary wave [4]. For example, the small horizontal scales and large amplitudes of these short waves mean that both wave orbital currents and current shear can become large, which can lead to instability and loss of wave energy by turbulent dissipation, and hence to mixing of the water column. This can subsequently lead to a thickening of the pycnocline [5]. Sandstrom and Elliot [6] have pointed out that the IW- associated vertical mixing may act like a "nutrient pump," supplying nitrates to the euphotic zone in the surface layer.

As mentioned, the shallow water, finite amplitude, 2-layer internal wave problem leads to the KdV equation. One begins with the equations for inviscid, incompressible flow (Euler's equation and continuity equation) and, through the perturbative method of multiple scales, arrives, to first order nonlinearity, at the KdV equation. If we include viscous effects, then we need to consider the Navier-Stokes equations, which can be written in our case as

$$\rho[\partial_t + \mathbf{u} \cdot \nabla]\mathbf{u} = -\nabla p + \mu \nabla^2 \mathbf{u}, \qquad\qquad 5)$$

and where μ is viscosity and the vector $\mathbf{u}$ is the fluid particle velocity.

These equations are different from the inviscid case by the addition of a dissipative (or diffusive) term $\mu \nabla^2 \mathbf{u}$. For our purposes, this term and the convective term $(\mathbf{u} \cdot \nabla)\mathbf{u}$, and their relative interplay, will be the most essential features we consider. The simplest 1-D model problem for representing convection/diffusion problems, or from our perspective, nonlinear dissipative wave phenomena, is Burgers equation [7]

$$u_t + u u_x = \mu u_{xx} \qquad\qquad 6)$$

where we retain μ to indicate the dissipation coefficient.

Upon comparing the KdV and Burgers equations, we note that, in the former case, the dissipative term is missing. In the latter case the dispersive term is missing. A natural generalization to weakly nonlinear, dispersive, dissipative systems is to consider the model problem:

$$u_t + u u_x + v u_{xxx} = \mu u_{xx} \qquad\qquad 7)$$

which is called the KdVB equation (see Ref. [7] for a bibliography of papers concerning this equation).

We proceed by considering the numerical solution of Eq. 7), where a $sech^2(x)$ function is used for an initial condition. Refer to Broadhead [2] for algorithmic details. In Fig. 2 we show the dissipative effect on a single solitary wave, where we overlay the first and last pulse, and where the latter has been scaled and shifted for comparison purposes. The effect we primarily want to point out is the pulse broadening. In order to connect these simulations to physical scales, we assume an IW with a 9 m amplitude, with $\lambda = 150$ m, $\Delta \rho = 4$ kg/m^3, and an energy of 6.35×10^5 J/m. In order for the IW to dissipate to an amplitude of 5.6 m, which is the equivalent percentage loss we found in the KdVB simulation above, we need an energy loss of 3.87×10^5 J/m. If we assume that our solitary wave is traveling at an average speed of about 0.5 m/s, over a distance of ~10 km, and use a dissipation rate of 5×10^{-2} W/m^2, then the desired amplitude reduction will occur over a time interval of about 5 hours.

Acoustical Simulations

For linear acoustic wave propagation due to a harmonic point source in an azimuthally symmetric ocean waveguide, the appropriate wave equation governing the excess pressure p is the two-dimensional Helmholtz equation

$$\frac{\rho}{r}\frac{\partial}{\partial r}\left(\frac{r}{\rho}\frac{\partial p}{\partial r}\right) + \rho\frac{\partial}{\partial z}\left(\frac{1}{\rho}\frac{\partial p}{\partial z}\right) + \frac{\omega^2}{c^2_{(r,z)}}p = \frac{-\delta(z - z_s)\delta(r)}{2\pi r} \qquad\qquad 9)$$

where, in general, the density $\rho = \rho(r,z)$ is a function of range and depth, as is c, the sound speed. The point source, located at the r-origin at depth z_s, has harmonic time dependence $\exp(-i\omega t)$, where $\omega = 2\pi f$, and f is frequency in Hz. The normal mode model KRAKENC [8] was used to obtain one-way (outgoing) solutions to Eq. 9) for the environmental parameters given in Fig. 1.

Two methods were employed: 1) adiabatic normal modes and 2) one-way coupled modes. The adiabatic normal mode solution is valid when the environmental parameters change sufficiently slowly, i. e., when mode coupling can be ignored. When mode coupling cannot be ignored, as is the case in examples shown later, a coupled mode approach can be used [8]. The environment is approximated by subdividing it into range-independent segments. Boundary conditions are then used to match the solutions at adjoining segment interfaces (i. e., continuity of pressure and radial particle velocity, respectively). Also needed are the source condition (r=0) and the Sommerfeld radiation condition (r→ ∞). This leads to a system of equations for the normal mode amplitudes, which can then be further simplified to a one-way (no backscattering) coupled mode formulation that allows an efficient range marching implementation [8]. In KRAKENC the full complex eigenvalue problem is solved. In order to include continuum approximations the leaky-mode approximation is utilized. These terms can be important when mode-coupling re-stimulates continuum contributions at potentially large source-to-receiver ranges r.

In Fig. 1, the acoustic environmental parameters are given, as well as the displacement of the thermocline that simulates the presence of a solitary internal wave. The given environment was input into KRAKENC and TL calculations were performed at a number of frequencies. We noticed various interesting phenomena, but concentrated on what occurred in the frequency band 900 Hz -- 1030 Hz.

Figure 3 shows the result of this calculation for a source depth of 25 m, which is below the thermocline. The topmost figure, represents the normal mode solution in the wave guide in the absence of an IW packet. When the IW is present, we have two choices of range dependent calculation with our model: 1) adiabatic normal modes and 2) coupled modes, which are displayed in the middle and bottom figures, respectively.

The propagation feature we call to the reader's attention is that, for this scenario, the coupled mode solution predicts an enhanced transfer of acoustic energy from below the thermocline into the mixed layer (ML) at least for propagation frequencies around 940 Hz and 1005 Hz. The fact that this phenomenon is missing in the adiabatic modes calculation is initial evidence that the IW is inducing mode coupling, which is, in turn, responsible for the energy

transfer phenomenon. We should also point out the similarity of the adiabatic normal mode and range-independent solutions for the cases presented. In Fig. 4, we take a more detailed look at the calculations by considering a horizontal slice through the 2-D TL surfaces in Fig. 3. The energy transfer already mentioned is evident.

In Fig. 5, we display the results of calculations for TL vs. frequency, where the dashed curve is produced by differencing the TL for coupled modes and the range-independent case. We observe a doublet resonance structure at 940 Hz and 1005 Hz. We are now able to pose a specific question as regards the effects of dissipation on the acoustic resonance structure we have identified: how would the peak broadening due to dissipation affect the acoustical resonant structure shown by the dashed curve. Using a new acoustical environment in which we have approximately doubled the IW length scale, we repeat the calculations to produce the new resonance peaks shown by the solid curve. Note, the structure, slightly altered, is shifted up in frequency by about 25 Hz.

Mode Coupling Analysis

To study the nature of the mode coupling that is playing a role in the propagation we consider the modal amplitudes, defined by

$$a = U^H p \tag{10}$$

32

where **p** is a vector of pressures at a fixed range, **a** is a vector of modal amplitudes and **U** is a matrix whose columns are the appropriate (local) mode functions.

In Fig. 6, we display the modal amplitude calculated from the vertical pressure at the 1500 m range for 940 Hz. There are several points to note: 1) three modes, modes 1, 3, and 5, dominate the propagation in the range-independent case, and 2) these three modes carry less energy when the IW is present (and mode coupling is allowed), whereas the higher modes are enhanced (especially mode 8). This suggests a coupling of modes 1, 3, and/or 5 to at least mode 8. Further evidence of this can be seen in Fig. 7 where we display the modes in question. Modes 1, 3, and 5 are largely confined to the wave guide region between the ML and the water bottom. However, mode 8, which is stimulated by the IW at the expense of the other three, has a large component in the ML.

Following a procedure analogous to that used by Zhou *et al.* [2], we can make use of mode coupling theory to tie the characteristic spatial scales of the IW packets to the normal mode spatial scales represented by horizontal wave numbers. This theory predicts significant coupling between modes that obey the relation

$$k_{int} \approx k_m - k_n \qquad \qquad 11)$$

where k_m and k_n are the horizontal wave numbers corresponding to the mth and n^{th} modes, and k_{int} is the wave number corresponding to the appropriate length scale for an internal wave. By eye, we chose two length scales that bracketed the main solitary wave shown in Fig. 1, shown in Fig. 8. The scales correspond to the following wave number interval: $[k_{150m}, k_{60m}] \approx [0.042, 0.105]$. Horizontal wave numbers obtained from KRAKENC for modes 1, 3, 5 and 8 obey: $\Delta k_{1,8} \approx 0.084$, $\Delta k_{3,8} \approx 0.071$, and $\Delta k_{5,8} \approx 0.045$, which fall within the given wave number range for the IW. This indicates a general consistency with mode coupling theory for our main solitary wave. It also confirms the role that coupling of modes 1, 3, and 5 to mode 8 plays in the effect.

Simple Model for Predicting Resonance Properties

Along with the relation $\lambda_{int} = 2\pi / k_{int}$ and Eq. 11), we can write

$$\lambda_{int} \approx 2\pi / |k_m(\omega_R) - k_n(\omega_R)| . \qquad \qquad 12)$$

Using some means of computing various (m,n) horizontal wave number pairs, we can determine the associated resonant frequency ω_R for a given length scale, based on the

particular mode coupling theory implied by Eq. 11). The simplest case is for a rigid bottom, isovelocity waveguide, which provides an analytical relation:

$$k_m^2 = (\tfrac{\omega}{c})^2 - \left([m - \tfrac{1}{2}] \tfrac{\pi}{H} \right)^2, \ m = 1, 2, \dots N \qquad \qquad 13)$$

Curves produced with these albeit simple assumptions are shown in Fig. 9 for various mode pairs. We should only interpret these curves qualitatively, and only in so far as they agree with what we have already learned from simulations. It should be pointed out that the curves predict two features we have already noted: 1) an increase in the resonant frequencies for an increase in the IW length scale (at least for our present scenario), and 2) a multiplet line structure, since, in

33

general, unique frequencies are associated with different (m,n) pairs (although there is some degeneracy and fine structure).

Discussion and Conclusions

In the present work, mode coupling theory has been use to produce a simple model of the connection between acoustic resonance frequencies and internal wave length scale. This model, which explicitly includes several acoustical environmental parameters, qualitatively correctly predicts two of the effects we observed so far in simulations: namely, 1) an increase in acoustic resonant frequency with an increase in the IW length scale, and 2) prediction of a multiplet line structure due to a generally unique frequency being associated with each (m,n) mode pair. This result should, at best, be thought of as only a first crude attempt at a general approach to solitary internal wave acoustic resonance spectroscopy. We are currently refining the analysis, and of course, all such theories and models are ultimately required to be validated by experimental measurements. Such measurement programs are currently under way, one of which the authors are participating in.

References

[1] J. Zhou, X. Zhang and P. H. Rogers, "Resonant interaction of sound wave with internal solitons in the coastal zone, *J. Acoust. Soc. Am.*, Vol. 90, pp. 2042-2054, 1991.

[2] M. K. Broadhead, M. K., Resonant transfer of acoustic energy into the mixed layer by internal solitons," *J. Acoust. Soc. Am.*, Submitted, 1995.

[3] L. A. Ostrovsky and Yu. A. Stepanyants, "Do internal solitons exist in the ocean?," *Rev. Geophys.*, Vol. 27, pp. 293-310, 1989.

[4] H. Sandstrom and N. S. Oakey, "Dissipation in internal tides and solitary waves," *J. Phys. Oceanogr.*, Vol. 25, pp. 604-614, 1995.

[5] D. Bogucki and C. Garrett, "A simple model for the shear-induced decay of an internal solitary wave," *J. Phys. Oceanogr.*, Vol. 23, pp. 1767-1776, 1993.

[6] H. Sandstrom and J. A. Elliot, "Internal tide and solitons on the Scotian Shelf: a nutrient pump at work," *J. Geophy. Res.*, Vol. 89, pp. 6415-6426, 1984.

[7] A. Jeffrey and T. Kakutani, "Weak nonlinear dispersive waves: a discussion centered around the Korteweg-de Vries equation," *SIAM Review*, Vol. 14. No. 4, pp. 582-643, 1972.

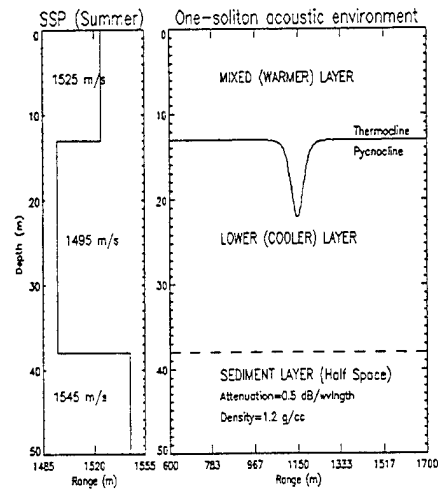[8] M. B. Porter, "The KRAKEN normal mode program," SACLANTCEN Memorandum SM-245 (September 1991).

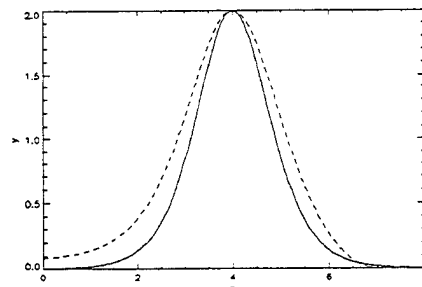FIG. 1. Acoustic environment showing the 1-soliton IW simulation.

FIG. 2. KdVB evolution for $\mu=0.01$, $t_f=5.6$. Overlay of first pulse (solid) and last (dashed). Dashed curve has been shifted and scaled for clarity.
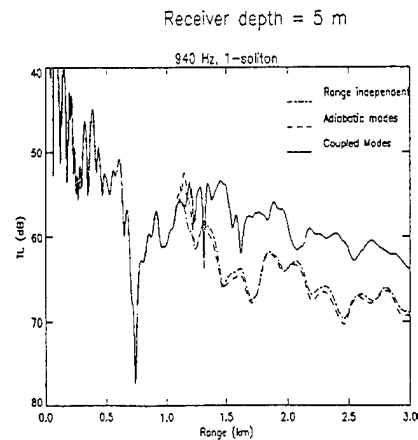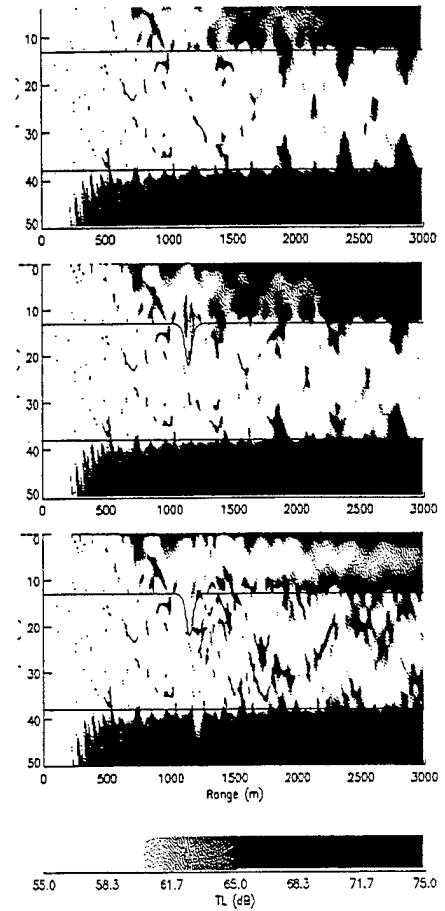

FIG. 3. Comparison of TL for 1-soliton environment at 940 Hz: range independent (topmost figure), adiabatic modes (middle), and coupled modes (bottom).
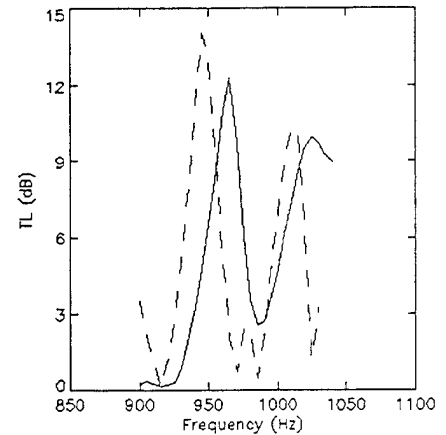

FIG. 4. Horizontal TL slices at receiver depth of 5 m corresponding to Fig. 2. Curves for range independent, adiabatic and coupled modes are shown.

FIG. 5. (Dashed) ΔTL versus frequency for a receiver at a depth of 5 m and range = 1500 m. Peaks are at 940 Hz and 1005 Hz. (Solid) Resonance curve for broadened IW.
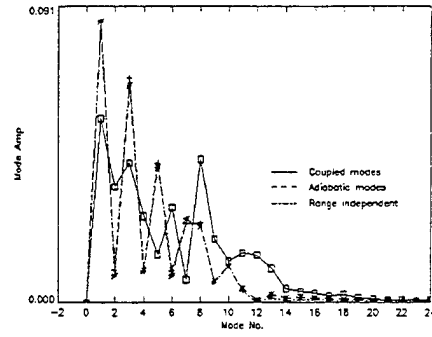
35

FIG. 6. Modal amplitudes for vertical pressures at range = 1500 m. Solid indicates coupled modes for IW's present. Dash-dot indicates absence of IW's.
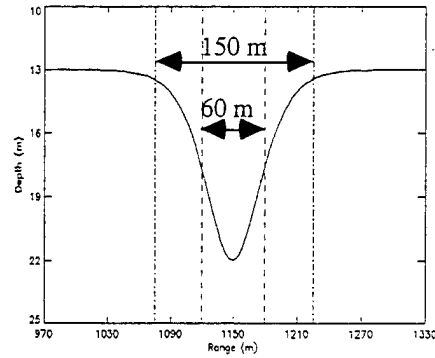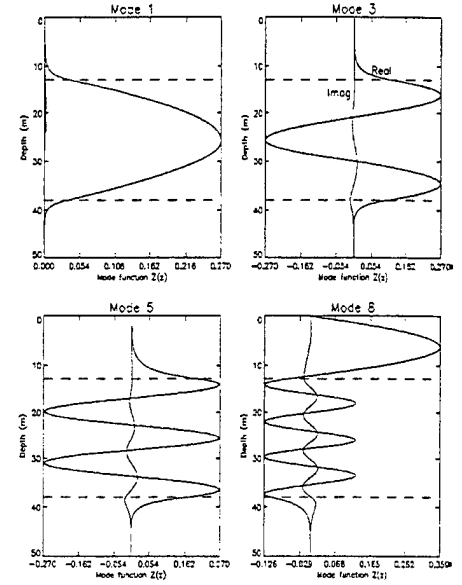

FIG. 7. Mode functions 1, 3, 5, and 8 for receiver range 1500 m. Note, modes 1, 3, and 5 are mainly confined to below the mixed layer, while mode 8 has a larger concentration of energy in the mixed layer.

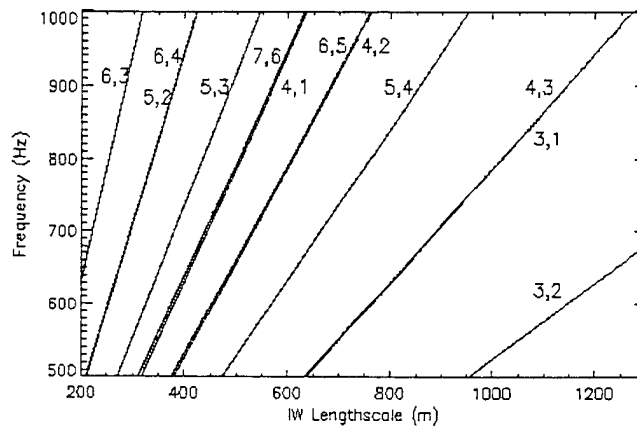FIG. 8. Length scale bounds associated with the main solitary wave.

FIG. 9. Curves produced using Eqs. 12 and 13 showing the relationship between resonant frequency and IW length scale.